CHEMISTRY OF THE ORPHAN STREAM I: IDENTIFYING STREAM MEMBERS FROM LOW-RESOLUTION SPECTROSCOPY

Andrew R. Casey[1,2], Stefan C. Keller[1], Gary Da Costa[1], Elizabeth Maunder[1]
Draft version September 15, 2012

ABSTRACT

We present coordinates and properties of candidate K giant members in the Orphan Stream, which have been identified from low resolution spectroscopic data taken with AAOmega on the Anglo-Astronomical Telescope. With modest S/N and independent cuts in photometry, kinematics, gravity and metallicity we yield self-consistent, highly probable stream members. Our data indicates an overall stream metallicity of [Fe/H] = −1.71 with an intrinsic dispersion of $\sigma = 0.56$ dex which is more metal-rich than previously found and unbiased by spectral type. The metallicity dispersion in our stream sample suggests that the unidentified Orphan Stream parent is a dSph satellite. We find a revised stream distance of 23.5 ± 1.0 kpc near the celestial equator, and our kinematic signature peaks at $V_{GSR} = 00.0$ km s^{-1}. The observed velocity dispersion of our highest probability members is consistent with arising from the velocity uncertainties alone, indicating that at least along the line-of-sight, the Orphan Stream is kinematically quite cold. We highlight likely members for high resolution spectroscopic follow-up.

Subject headings: Galaxy: halo, structure — Individual: Orphan Stream — Stars: K-giants

1. INTRODUCTION

The Milky Way stellar halo has partly formed through the accretion of satellites which are disrupted by tidal forces as they fall into the Milky Way's potential. Stars which were once gravitationally bound to the satellite are left behind in a stream of stars. Stream kinematics are sensitive to the shape of the galactic potential, allowing us to constrain the Milky Way potential, and reconstruct the formation history of the Milky Way. The level of accreted substructure in the Milky Way has only recently become apparent through multi-band photometric surveys like the Sloan Digital Sky Survey (SDSS). The more prominent of the detectable substructures, like Sagittarius, have been well-studied. One of the more prominent – yet less studied – substructures is that of the Orphan Stream.

The Orphan Stream was independently detected by both Grillmair & Dionatos (2006) and Belokurov et al. (2006), and is distinct from other substructures in the halo. The stream stretches over 60 ° in the sky, has a low surface brightness and a narrow stream width of only ∼2 ° and as the name suggests, the parent object largely remains a mystery. The stream extends past the celestial equator – outside the SDSS footprint – but has not been detected in existing southern surveys (Newberg et al. 2010). Whilst the parent system remains elusive, significant effort has been placed on associating the stream with known Milky Way satellites (Zucker et al. 2006; Fellhauer et al. 2007; Jin & Lynden-Bell 2007; Sales et al. 2008). In contrast, there has been relatively limited observational work on the Orphan Stream itself other than the original discovery papers (Grillmair & Dionatos 2006;

Belokurov et al. 2006, 2007) and the work of Newberg et al. (2010). This is largely to be expected given the absence of multi-band photometry in the southern sky and the low total luminosity of the stream, making it difficult to reliably separate Orphan Stream members from halo stars. Further understanding on the extent of the stream awaits the SkyMapper and Pan-STARRS photometric surveys (Keller et al. 2007; Hodapp et al. 2004).

As Sales et al. (2008) point out, there is a natural observational bias towards more massive and recent mergers like Sagittarius. Consequently, the fainter end of this substructure distribution has yet to be fully recovered, or thoroughly examined. Interestingly, there are indications that some fainter substructures like the Orphan Stream and the Palomar 5 tidal tails (Odenkirchen et al. 2009) have orbits which seem to be best-fit by Milky Way models with nearly 60% less mass (Newberg et al. 2010) than generally reported by Xue et al. (2008) and Koposov et al. (2010). Such a discrepancy in the mass of the Milky Way is troublesome. More complete photometric and kinematic maps of these low total luminosity streams may provide the best test as to whether this mass discrepancy is real, or an artefact of incomplete observations. Whilst the full spatial extent of the stream remains incomplete, we can examine the detailed chemistry of its members and investigate the stream history, as well as make predictions about the nature of the host system.

In this letter we present a detailed, self-consistent analysis to identify K giant members of the Orphan Stream. Using our selection method we have catalogued the locations of ten highly probable Orphan Stream candidates, all worthy of high-resolution spectroscopic follow up. In the following section we outline our photometric target selection. In §3 we describe the low-resolution spectroscopic observations. The data analysis, including stream identification, is discussed in §4 and in §5 the conclusions, predictions and future work are presented.

[1] Research School of Astronomy & Astrophysics, Australian National University, Mount Stromlo Observatory, via Cotter Rd, Weston, ACT 2611, Australia; acasey@mso.anu.edu.au
[2] Massachusetts Institute of Technology, Kavli Institute for Astrophysics and Space Research, 77 Massachusetts Avenue, Cambridge, MA 02139, USA

2. TARGET SELECTION

We have targeted K giant members of the Orphan Stream in order to investigate their detailed chemistry. Because K-giants are difficult to unambiguously detect from photometry alone, low-resolution spectroscopy is required to estimate stellar parameters and determine radial velocities. The Orphan Stream has a low spatial over-density on the order of $\sim 10\%$, which makes it difficult to separate stream members from halo stars. However, there is a well described distance gradient along the stream (Belokurov et al. 2007; Newberg et al. 2010) which provides an indication on where we should focus our spectroscopic efforts.

The Orphan Stream is closest to us in two locations on the edge of the SDSS footprint: at the celestial equator (Belokurov et al. 2007), and along outrigger SEGUE Stripe 1540 (Newberg et al. 2010). These two locations are unequivocally the best place to recover bright stream members. We have targeted two fields centered on $(\alpha, \delta) = (10:48:15, 00:00:00)$ and $(10:48:15, -02:30:00)$, and employed a combination of colour cuts with the SDSS DR 7 (Abazajian et al. 2009) data set in order to identify likely K giants:

$$0.6 < (g - i)_0 < 1.7 \tag{1}$$
$$-15(g - i)_0 + 27 < \quad g_0 \quad < -3.75(g - i)_0 + 22.5 \tag{2}$$
$$15 < \quad i_0 \quad < 18 \tag{3}$$

Given our colour selection we expect to recover giants, and dwarf contaminants. The lack of 2MASS photometry for the selected stars means we cannot use the $(J-H, H-K)$ diagram to aid the separation of candidate giants from contaminating dwarfs.

3. OBSERVATIONS

Observations took place on the Anglo-Astronomical Telescope using the AAOmega spectrograph in April 2009. AAOmega is a fibre-fed, dual beam multi-object spectrograph which is capable of simultaneously observing spectra of 392 (science and sky) targets across a $2°$ field of view. We used the $5700\,\text{Å}$ dichroic in combination with the 1000I grating in the red arm, and the 580V grating in the blue arm. This provides a spectral coverage between $800 \leq \lambda \leq 950\,\text{nm}$ in the red at $\mathcal{R} \approx 4400$, and between $370 \leq \lambda \leq 580\,\text{nm}$ with a lower resolving power of $\mathcal{R} \approx 1300$ in the blue.

The data were reduced using the standard 2DFDR reduction pipeline[3]. After flat-fielding, throughput calibration for each fibre was achieved using the intensity of skylines in each fibre. The median flux of dedicated sky fibres was taken for sky subtraction, and wavelength calibration was performed using arc lamp exposures between science frames. Three thirty minute science exposures were median combined to assist with cosmic ray removal. The median S/N obtained in the red arm for our fields is modest at 35 per pixel. With the presence of strong Ca II triplet lines in the red arm we are able to ascertain reliable radial velocities and reasonable estimates on overall metallicity (Starkenburg et al. 2010, and references therein). Our spectral region also includes gravity-sensitive magnesium lines: Mg I at $8807\,\text{Å}$, and the Mg I b $3p$-$4s$ triplet lines at $\sim 5178\,\text{Å}$. As we demonstrate in the next section, these lines are sufficient to discriminate dwarfs from giants even with weak signal.

The blue and red arm spectra were normalised using a third order cubic spline after multiple iterations of outlier clipping. We used defined knot spacings of 20 nm in the red arm, and 5 nm in the blue arm in order to accommodate often poor S/N, and varying strengths of molecular band-heads.

4. ANALYSIS

We have employed a combination of separate criterion to identify likely Orphan Stream members: kinematics, a giant/dwarf indication from Mg I lines, and consistent metallicities from isochrone fitting and the Ca II triplet lines. Each criterion is discussed here separately.

4.1. Kinematics

Radial velocities were measured by cross-correlating our normalised spectra against a K-giant synthetic template with a temperature of $4500\,\text{K}$, $\log g = 1$ and $[\text{Fe/H}] = -1.5$ across the range $845 \leq \lambda \leq 870\,\text{nm}$. Heliocentric velocities were translated to the galactic rest frame by adopting the local standard of rest velocity as $220\,\text{km s}^{-1}$ towards $(l, b) = (53°, 25°)$ (Kerr & Lynden-Bell 1986; Mihalas & Binney 1981)[4]. Newberg et al. (2010) presented a comprehensive kinematic dataset on the Orphan Stream using BHB stars and employed a slightly different galactocentric transformation. This systematic difference equates to our galactocentric rest frame velocities being on average $\sim 5\,\text{km s}^{-1}$ lower than those of Newberg et al. (2010).
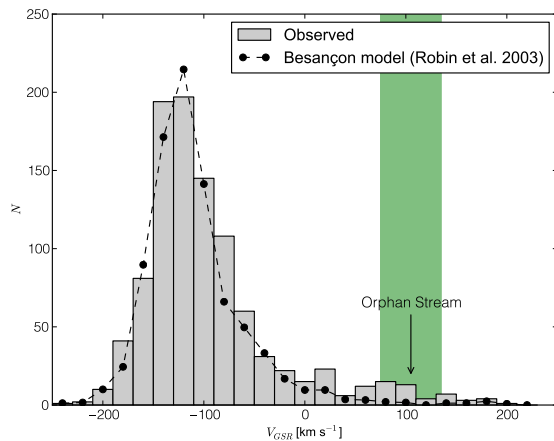

FIG. 1.— Galactocentric rest frame velocities for stars in both our observed fields (grey), and predicted Besançon velocities which have been scaled to match our observed sample size. The expected kinematic signature from Newberg et al. (2010) for the Orphan Stream is highlighted, as is our kinematic selection window (green).

Figure 1 shows a histogram of our galactocentric velocities, compared to the predicted smooth line-of-sight velocity distribution for this region from the Besançon model (Robin et al. 2003). We have selected predicted

[4] Where $V_{GSR} = V_{\text{HELIO}} + 220 \sin l \cos b + 16.5 \times [\sin b \sin 25 + \cos b \cos 25 \cos (l - 53)]$

stars from the Besançon model using the same criterion outlined in §2 after using the Jordi et al. (2006) colour transformations. It is clear that our target selection has yielded mostly nearby thick disk dwarf stars with $V_{GSR} \approx -120 \, \mathrm{km \, s^{-1}}$. The expected kinematic signature for the Orphan Stream, as Newberg et al. (2010) reported, is labelled in Figure 1. There is no sharp kinematic peak representative of the Orphan Stream exists in our sample. From kinematics alone, our targets appears largely indistinguishable from a smooth halo distribution.

In this region Newberg et al. (2010) found the Orphan Stream to have $V_{GSR} = 110 \, \mathrm{km \, s^{-1}}$ from BHB stars, approximately $105 \, \mathrm{km \, s^{-1}}$ on our scale. To isolate potential Orphan Stream members we have nominated a relatively wide kinematic selection region between $75 \leq V_{GSR} \leq 135 \, \mathrm{km \, s^{-1}}$, which yields twenty-five Orphan Stream candidates. The typical uncertainty in our kinematics is $\pm 5.0 \, \mathrm{km \, s^{-1}}$, although for our fainter targets this quickly increases above $10 \, \mathrm{km \, s^{-1}}$.

4.2. *Dwarf/Giant Discrimination*

We have measured the equivalent widths of the gravity-sensitive Mg I line at 8807 Å to distinguish dwarfs from giants (Battaglia & Starkenburg 2012). At a given temperature (or $g - r$) and metallicity, giant stars present narrower Mg I absorption lines than their dwarf contaminants. Given our target selection, our sample is likely to contain many more dwarfs than giants. In some cases no Mg I 8807 Å line was apparent, so an upper limit was estimated based on the S/N. In these cases the candidate was considered a "non-dwarf" because we cannot exclusively rule out a metal-poor sub-giant with this criterion alone. For these purposes we are only looking for a simple indication as to whether a star is likely a dwarf or not. Figure 2 illustrates the trend with $\mathrm{EW}_{\lambda 8807}$ against SDSS de-reddened[5] $g - r$, illustrating the dominant upper dwarf branch we wish to exclude. The adopted dwarf/giant separation line is shown. Admittedly this selection criterion is not particularly strict, but we are allowing multiple inclusive cuts and taking the intersection of these criteria to identify Orphan Stream giants.

This analysis was also performed using the total equivalent width of the Mg I b triplet lines. Both analyses were entirely consistent with each other: essentially the same candidate selection was found using both techniques. However, given slightly poorer signal at the Mg I b triplet, we were forced to adopt many more upper limits than when using the 8807 Å line. Because we classify all upper limits as being "non-dwarfs" (i.e. potential OSS giants), we deduced a slightly larger candidate sample for the Mg I b analysis, which was primarily populated by upper limits. In conclusion, we found the Mg I line at 8807 Å appeared to be a more consistent dwarf discriminant given our weak S/N – particularly for our fainter stars – and thus we have used the 8807 Å Mg I selection throughout the rest of our analysis.

Our dwarf/giant separation line in Figure 2 yields 425 potential giants. This fraction of giants (~44%) is much larger than what would be expected given our selection

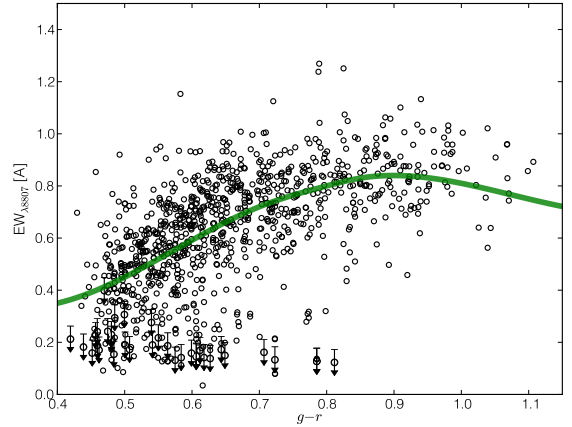[5] All magnitudes presented in this letter are de-reddened using the Schlegel et al. (1998) dust maps.

FIG. 2.— SDSS $g - r$ against the measured equivalent width of the Mg I transition at 8807 Å. Dwarf contaminants occupy the more populous upper branch. Our separation line between dwarfs and giants is shown in green.

criterion (e.g. see Casey et al. 2012a). Hence, our gravity criterion is extremely inclusive and susceptible to dwarf contamination. Upon taking the intersection of our kinematic and gravity selections, we deduce eighteen stars that appear likely Orphan Stream K giants.

4.3. *Metallicities*

We have measured the equivalent widths of the Ca II near-infrared triplet lines for stars that meet our kinematic and surface gravity criteria. After correcting for luminosity, the equivalent width of the Ca II triplet lines provide a good indication of the overall metallicity of a RGB star (Armandroff & Da Costa 1991). We have employed the Starkenburg et al. (2010) relationship and corrected for luminosity in g against the horizontal branch magnitude at $g_{HB} = 17.1$ (Newberg et al. 2010). Strictly speaking, the Ca II–[Fe/H] calibration is only valid for stars brighter than the horizontal branch, although the relationship only becomes significantly inappropriate near $g - g_{HB} \sim +1$ (Saviane et al. 2012). Many of our candidates are fainter than this valid luminosity range, and therefore they should not be excluded solely because of their derived metallicities. Stars fainted than g_{HB} will have slightly lower metallicities than predicted by our Ca II–[Fe/H] relationship, and for these stars we will only use metallicities to assign a relative qualitative likelihood for stream membership. Given a distance to the Orphan Stream, we can also estimate a star's metallicity through isochrone fitting. We have used a 10 Gyr Marigo et al. (2008) isochrone at 21.4 kpc (Newberg et al. 2010) and found metallicities for all eighteen likely stream members from their best-fitting isochrone (see Figure 3). Derived metallicities from Ca II line strengths and isochrone fitting that are consistent (within ± 0.3 dex) indicates these measurements are reliable, and that these stars are indeed at a distance of ~21.4 kpc. We find ten highly likely stream members with consistently derived metallicities. They fall within the shaded region illustrated in Figure 3.

We have adopted a final overall metallicity for each star based on the quality of our [Fe/H] measurements. Adopted values are tabulated in Table 1. From our

ten highly likely stream members we find an overall stream metallicity of [Fe/H] = −1.71 with a dispersion of σ = 0.56 dex. This abundance spread is larger than typically seen in globular cluster stars and is more representative of the chemical spreads seen in dSph satellites. Newberg et al. (2010) found a stream metallicity of [Fe/H] = −2.1 from BHB stars, which is not inconsistent with our measurement given the spread in Orphan Stream K-giant metallicities.
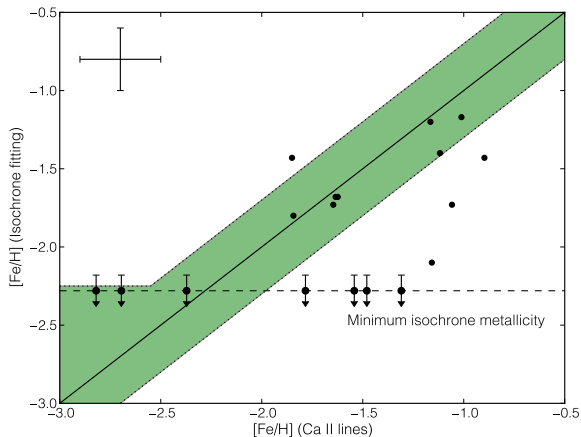

Fig. 3.— Metallicities from the Ca II triplet lines versus those found from fitting isochrones to the eighteen stars that meet our kinematic and surface gravity criteria. Both abundance determinations imply these stars are RGB members of the Orphan Stream at a distance of ∼21.4 kpc (Newberg et al. 2010). Consistency between these methods indicates highly likely stream membership (green region). The minimum isochrone metallicity, and a representative uncertainty of 0.2 dex for abundance measurements is shown.

Given that our Orphan Stream giants cover a wide evolutionary range along the giant branch (Figure 4), we are in a good position to revise the distance estimate to the stream. Given a 10 Gyr Marigo et al. (2008) isochrone at [Fe/H] = −1.71, we find a best-fitting distance to the stream of 23.5 ± 1.0 kpc at $(l,b) = (250\,^\circ, 50\,^\circ)$. This isochrone is also shown in Figure 4, and it is clear that the four most probable member stars lie almost precisely on this isochrone. Our derived distance is slightly farther than the 21.4 ± 1.0 kpc found by Newberg et al. (2010), although given the difficulty in measuring distances these values are largely in agreement.

5. CONCLUSION

We have presented a detailed analysis to isolate individual Orphan Stream K giants from low-resolution spectroscopy using a combination of photometric, kinematic, gravity, and metallicity information. Although each individual criterion is likely to induce some level contamination, their intersection reveals ten highly probable, self-consistent, Orphan Stream K giants. We deduce a median stream metallicity of [Fe/H] = −1.71 and find an intrinsically wide metallicity spread of σ = 0.56 dex, indicative of a dSph origin. Unlike other stellar tracers, K-type giants can exist at all metallicities, hence our derived metallicity spread is likely representative of the true stream metallicity distribution function. Recall that
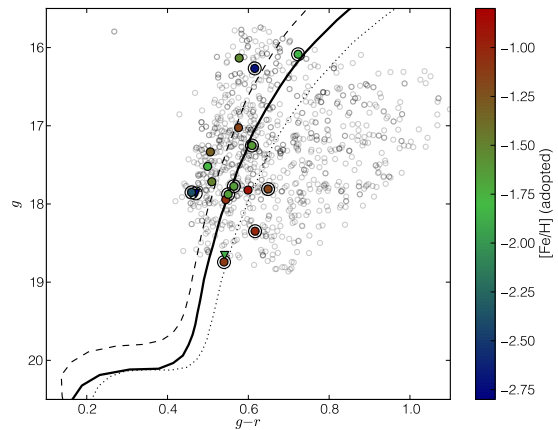

Fig. 4.— Color magnitude diagram showing our observed candidates (grey). Observations fulfilling kinematic and gravity cuts are colored by their metallicity, and those with upper limits for surface gravity are marked as triangles (▽). Highly probable stream members with consistent line strength- and isochrone-derived metallicities are circled. Relevant 10 Gyr Marigo et al. (2008) isochrones at [Fe/H] = −1.5 (dotted), −2.0 (dashed) at 21.4 kpc (Newberg et al. 2010) are shown, as well as our best-fitting 10 Gyr isochrone of [Fe/H] = −1.71 at 23.5 kpc (solid).

the metallicity determination was performed after kinematic and gravity cuts, and our most probable members lay perfectly on a 10 Gyr isochrone of [Fe/H] = −1.71. Our stream members indicate a revised distance to the stream of 23.5 ± 1.0 kpc at $(l, b) = (250\,^\circ, 50\,^\circ)$, slightly farther than that deduced by Newberg et al. (2010).

If the Orphan Stream continues through SEGUE Stripe 1540 at $(l, b) = (271\,^\circ, 38\,^\circ)$ as Newberg et al. (2010) found, then the stream is even closer there than in the region analysed here. Thus, if our observations and analyses are repeated at $(271\,^\circ, 38\,^\circ)$, we predict K giant stream members of brighter apparent magnitude will be recovered. If the stream density is similar to or higher than what we observe at $(l, b) = (250\,^\circ, 50\,^\circ)$ then more K giant Orphan Stream members are likely to be recovered in the Stripe 1540 field.

Using a maximum-likelihood estimation we find the stream velocity at $(l, b) = (250\,^\circ, 50\,^\circ)$ from five stars to be $V_{GSR} = 00.0 \pm 0.0$ km s^{-1} and the intrinsic dispersion to be 0.0 ± 0.0 km s^{-1}, i.e., comparable to our velocity resolution and consistent with zero. If we exclude five stars with weak signal – and hence large velocity uncertainties – this dispersion is found to be 0.0 ± 0.0 km s^{-1}. These velocities indicate that the Orphan Stream is a very cold stream, and implies their motion is largely perpendicular to the line of sight.

The K giants presented here can provide great insight into the chemistry, and history of the Orphan Stream. High-resolution spectroscopic observations have been taken for our most highly probable members and a detailed chemical analysis will be presented in a forthcoming paper (Casey et al. 2012c, in prep.). Detailed chemical abundances can help determine both the nature of the host system before it's discovered, and allows us to compare peculiar chemical signatures with those of the known Milky Way satellites in order to associate likely parents. However, at least for the moment, the Orphan Stream remains appropriately named.

TABLE 1
Identified Orphan Stream Candidates

α (J2000)	δ (J2000)	g	$g - r$	V_{hel} (kms^{-1})	V_{GSR} (km s^{-1})	V_{err} (km s^{-1})	$EW_{\lambda 8807}$ (Å)	$[Fe/H]_{Ca}$ (dex)	$[Fe/H]_{iso}$ (dex)	$[Fe/H]^a$ (dex)	Stream Prob.
10:46:21.9	+00:43:21.8	17.52	0.50	209.2	73.3	9.3	0.273	−1.78	<−2.28	−1.78	Low
10:46:29.3	−00:19:38.5	17.77	0.56	217.4	78.4	5.2	0.126	−1.63	−1.68	−1.63	High
10:46:50.4	−00:13:15.6	17.33	0.51	215.5	77.0	4.0	0.416	−1.31	<−2.28	−1.31	Low
10:47:06.1	−01:56:03.9	18.74	0.54	218.4	74.9	17.6	0.452	:−1.12[b]	−1.40	−1.40	High
10:47:15.0	−03:15:03.9	18.66	0.54	256.8	109.5	9.0	<0.19	:−1.85[b]	−1.43	−1.43	Medium
10:47:17.6	+00:25:07.7	16.09	0.72	215.7	79.2	3.3	0.212	−1.84	−1.80	−1.84	High
10:47:29.1	−02:02:22.6	17.86	0.47	236.9	93.2	29.8	<0.40	−2.82	<−2.28	−2.82	High
10:47:30.1	−00:01:24.5	17.25	0.61	221.3	83.6	3.5	0.123	−1.62	−1.68	−1.62	High
10:48:20.9	+00:26:34.4	17.88	0.55	254.9	118.9	11.7	0.467	−1.65	−1.73	−1.65	High
10:48:27.8	+00:55:24.0	17.72	0.51	259.1	124.5	6.7	0.182	−1.48	<−2.28	−1.48	Low
10:48:31.9	+00:03:35.7	17.02	0.58	242.3	105.1	5.1	0.234	−1.12	−2.10	−1.12	Low
10:48:44.4	−02:53:08.8	18.35	0.62	253.9	108.2	9.0	0.183	:−1.01[b]	−1.17	−1.17	High
10:48:46.9	−00:32:27.8	17.85	0.46	248.2	109.3	8.1	0.324	−2.37	<−2.28	−2.37	High
10:49:08.3	+00:02:00.2	16.27	0.62	218.5	81.5	4.6	0.034	−2.70	<−2.28	−2.70	High
10:50:13.1	+00:33:52.7	16.13	0.58	229.7	94.7	5.1	0.391	−1.54	<−2.28	−1.54	Low
10:50:24.2	−01:49:05.4	17.94	0.54	252.0	109.9	25.4	0.151	−1.06	−1.73	−1.06	Low
10:50:33.8	+00:12:19.1	17.82	0.60	233.5	97.5	5.9	0.596	−0.90	−1.43	−0.90	Medium
10:51:19.7	+00:05:15.5	17.81	0.65	218.7	82.7	5.0	0.198	−1.16	−1.20	−1.16	High

[a] Final adopted [Fe/H] value based on quality of two metallicity measurements.
[b] Sufficiently fainter than g_{HB} to qualify this measurement as uncertain.

REFERENCES

Abazajian, K. N., et al. 2009, ApJS, 182, 543
Armandroff, T. E., & Da Costa, G. S. 1991, AJ, 101, 1329
Battaglia, G., & Starkenburg, E. 2012, A&A, 539, A123
Belokurov, V., et al. 2006, ApJ, 642, L137
—. 2007, ApJ, 658, 337
Casey, A. R., Keller, S. C., & Da Costa, G. 2012, AJ, 143, 88
Fellhauer, M., et al. 2007, MNRAS, 375, 1171
Grillmair, C. J., & Dionatos, O. 2006, ApJ, 643, L17
Hodapp, K. W., et al. 2004, Astronomische Nachrichten, 325, 636
Jin, S., & Lynden-Bell, D. 2007, MNRAS, 378, L64
Jordi, K., Grebel, E. K., & Ammon, K. 2006, A&A, 460, 339
Keller, S. C., et al. 2007, PASA, 24, 1
Kerr, F. J., & Lynden-Bell, D. 1986, MNRAS, 221, 1023
Koposov, S. E., Rix, H.-W., & Hogg, D. W. 2010, ApJ, 712, 260
Marigo, P., Girardi, L., Bressan, A., Groenewegen, M. A. T., Silva, L., & Granato, G. L. 2008, A&A, 482, 883
Mihalas, D., & Binney, J. 1981, Science, 214, 829

Newberg, H. J., Willett, B. A., Yanny, B., & Xu, Y. 2010, ApJ, 711, 32
Odenkirchen, M., Grebel, E. K., Kayser, A., Rix, H.-W., & Dehnen, W. 2009, AJ, 137, 3378
Robin, A. C., Reylé, C., Derrière, S., & Picaud, S. 2003, A&A, 409, 523
Sales, L. V., et al. 2008, MNRAS, 389, 1391
Saviane, I., Da Costa, G. S., Held, E. V., Sommariva, V., Gullieuszik, M., Barbuy, B., & Ortolani, S. 2012, A&A, 540, A27
Schlegel, D. J., Finkbeiner, D. P., & Davis, M. 1998, ApJ, 500, 525
Starkenburg, E., et al. 2010, A&A, 513, A34
Xue, X. X., et al. 2008, ApJ, 684, 1143
Zucker, D. B., et al. 2006, ApJ, 650, L41